



OPEN ACCESS

EDITED BY

Giovanni Provenzano,
University of Trento, Italy

REVIEWED BY

Wei-Guang Li,
Fudan University, China
Aislinn Joanmarie Williams,
The University of Iowa, United States

*CORRESPONDENCE

Michael J. Schmeisser
✉ mschmeisser@uni-mainz.de

[†]These authors have contributed equally to this work and share first authorship

RECEIVED 02 April 2023

ACCEPTED 29 June 2023

PUBLISHED 21 July 2023

CITATION

Nardi L, Chhabra S, Leukel P, Krueger-Burg D, Sommer CJ and Schmeisser MJ (2023) Neuroanatomical changes of ionotropic glutamatergic and GABAergic receptor densities in male mice modeling idiopathic and syndromic autism spectrum disorder. *Front. Psychiatry* 14:1199097. doi: 10.3389/fpsy.2023.1199097

COPYRIGHT

© 2023 Nardi, Chhabra, Leukel, Krueger-Burg, Sommer and Schmeisser. This is an open-access article distributed under the terms of the [Creative Commons Attribution License \(CC BY\)](https://creativecommons.org/licenses/by/4.0/). The use, distribution or reproduction in other forums is permitted, provided the original author(s) and the copyright owner(s) are credited and that the original publication in this journal is cited, in accordance with accepted academic practice. No use, distribution or reproduction is permitted which does not comply with these terms.

Neuroanatomical changes of ionotropic glutamatergic and GABAergic receptor densities in male mice modeling idiopathic and syndromic autism spectrum disorder

Leonardo Nardi^{1†}, Stuti Chhabra^{1,2†}, Petra Leukel³, Dilja Krueger-Burg^{1,2}, Clemens J. Sommer^{2,3} and Michael J. Schmeisser^{1,2*}

¹Institute of Anatomy, University Medical Center of the Johannes Gutenberg-University, Mainz, Germany, ²Focus Program Translational Neurosciences, University Medical Center of the Johannes Gutenberg-University Mainz, Mainz, Germany, ³Institute of Neuropathology, University Medical Center of the Johannes Gutenberg-University, Mainz, Germany

Autism spectrum disorder (ASD) comprises a wide range of neurodevelopment conditions primarily characterized by impaired social interaction and repetitive behavior, accompanied by a variable degree of neuropsychiatric characteristics. Synaptic dysfunction is undertaken as one of the key underlying mechanisms in understanding the pathophysiology of ASD. The excitatory/inhibitory (E/I) hypothesis is one of the most widely held theories for its pathogenesis. Shifts in E/I balance have been proven in several ASD models. In this study, we investigated three mouse lines recapitulating both idiopathic (the BTBR strain) and genetic (*Fmr1* and *Shank3* mutants) forms of ASD at late infancy and early adulthood. Using receptor autoradiography for ionotropic excitatory (AMPA and NMDA) and inhibitory (GABA_A) receptors, we mapped the receptor binding densities in brain regions known to be associated with ASD such as prefrontal cortex, dorsal and ventral striatum, dorsal hippocampus, and cerebellum. The individual mouse lines investigated show specific alterations in excitatory ionotropic receptor density, which might be accounted as specific hallmark of each individual line. Across all the models investigated, we found an increased binding density to GABA_A receptors at adulthood in the dorsal hippocampus. Interestingly, reduction in the GABA_A receptor binding density was observed in the cerebellum. Altogether, our findings suggest that E/I disbalance individually affects several brain regions in ASD mouse models and that alterations in GABAergic transmission might be accounted as unifying factor.

KEYWORDS

ASD, autism, receptor autoradiography, ionotropic receptors, glutamate, GABA

Introduction

Autism Spectrum Disorder (ASD) is a complex neurodevelopmental condition involving altered social communication and presence of repetitive behaviour. Several other co-occurring conditions such as attention deficit hyperactivity disorder, depression, sleep disorder, epilepsy, anxiety, and intellectual disability are often associated with ASD (1). The prevalence of ASD has increased significantly in recent decades, with 1 in 100 children being affected across all socioeconomic, racial, and ethnic groups (2). Being a long-lasting condition, approximately 2% of the adult population is estimated to live with ASD (3). Although both genetic and environmental factors have been associated with ASD onset, its etiology still remains poorly understood. ASD is predominantly a heterogeneous disorder, majorly classified into syndromic and idiopathic forms. Syndromic cases are associated with clinically defined somatic and behavioral phenotypes. On the other hand, idiopathic forms have unknown etiology and account for the majority of ASD cases (4). However, synaptic dysfunctions remain a point of commonality among several disparate forms of autism (5).

Despite the neuroanatomical differences between humans and mice, some fundamental aspects of the neural mechanisms identified in animal models remain conserved across species and hence, translatable. Therefore, three well-renowned mouse strains characterized to study ASD features were chosen for this study. Black and tan brachyury (BTBR) mice are an inbred strain showing face validity for idiopathic ASD (6). Fragile X messenger ribonucleoprotein 1 (FMR1) is an mRNA binding protein mutated in fragile X syndrome, which is the most common cause of inherited intellectual disability and shares large degree of similarities in symptomatology with ASD. *Fmr1* knockout (KO) mice are the best characterized model to study fragile X syndrome. This model also shows promising behavioural and physiological features to be used as a validated model for ASD (7). SH3 and multiple ankyrin repeat domain 3 (SHANK3) is a key post-synaptic scaffolding protein, whose disruption is associated with the development of Phelan-McDermid Syndrome. *Shank3b* KO mice display key behavioral abnormalities associated with ASD (8).

Tight balance between excitatory and inhibitory synaptic transmission at neural circuits is crucial for normal brain development and function. Accordingly, shifts in the excitation/inhibition (E/I) balance have been implicated in the development and maintenance of ASD. In recent years, the theory of E/I imbalance in ASD has gained a lot of attention. It has been postulated that the autistic brain may be overactive because of a 'signaling imbalance' with too much excitatory signaling or too little inhibition at synaptic or circuit levels. This may also in part provide an explanation to the high propensity of people with ASD to develop seizures or epilepsy (9). Cumulative evidence now emerges to support the notion of E/I imbalances in various neurodevelopmental disorders including ASD in humans (10–15). Multiple factors such as synapse development, synaptic plasticity, intrinsic neuronal excitability, and intracellular signaling pathways play crucial roles in modulating E/I balance at cellular and circuit levels. However, it is important here to consider that the notion of "E/I balance" determining whether brain circuits are in homeostasis or not is vastly over simplified, since (A) microcircuits in different brain regions are not a unidirectional entity. They can be affected by different mixtures of excitation and inhibition inputs, (B) within a

single microcircuit, different sources of excitation and inhibition affect different aspects of neuronal functions, and (C) brain compensatory response for the imbalance should be also considered. A multitude of factors has a critical role in differentially contributing to regulate individual synapses, thereby contributing to the E/I imbalance (16). Novel modulators directed at restoring the E/I balance by mostly targeting synaptic ionotropic excitatory and inhibitory receptors, are proving a valuable tool and paving way to clinical trials (17).

Ionotropic receptors are ligand-gated ion channels, made up of multiple subunits. GABA_A (γ -aminobutyric acid, type A) is one of the main inhibitory receptors at synapses. There are in total 19 known subunits, which differentially combine in heteropentamers. Different subunits and their combinations contribute to the regional and functional diversity of the receptor, being most commonly composed of two alpha, two beta, and one gamma subunits (18). NMDA and AMPA receptors belong to the ionotropic glutamate receptors family. Functionally active NMDA receptors are heterotetramers composed of two obligatory GluN1 subunits along with two GluN2 or GluN3 subunits. Four different GluN2 and two different GluN3 subunits exist, adding up to the complex regional and developmental composition of the receptor (19). AMPA receptors are heterotetrameric combinations of the subunits GluA1, GluA2, GluA3, and GluA4 and are expressed throughout the brain. Being a highly dynamic receptor, trafficking, insertion, and removal of the GluA subunits at the synaptic membrane thus play major role in determining the efficacy of synaptic transmission (20). In this study, we investigated the binding profile to ionotropic excitatory glutamatergic and inhibitory GABAergic receptors in an age and region dependent fashion in three mouse models of ASD. Taken together, we show a convergent increase in the GABA_A receptor binding density at adulthood in dorsal hippocampus (DH), whereas reduced GABA_A receptor binding density was observed in the cerebellum (Cer) concomitantly. Quantitative evaluation of GABA_A, AMPA, and NMDA ionotropic receptor distribution will thus contribute to develop a better understanding towards underpinning the selective role of these receptors in alterations of E/I balance.

Materials and methods

Animals

BTBR (BTBR *T⁺ Itpr^{fl/fl}*, stock #002282), C57BL6/J (stock #000664), *Fmr1* (B6.129P2-*Fmr1^{tm1Cgr}/J*, stock #003025), and *Shank3b* (B6.129-*Shank3^{tm2Gfng}/J*, stock #017688) mice were purchased from Jackson laboratories and housed in a pathogen-free facility with 12 h light/dark cycle, food, and water available *ad libitum*. *Fmr1^{-/-}* (*Fmr1* KO) mice were generated by (21). *Shank3b* (B6.129-*Shank3^{tm2Gfng}/J*) mice were generated by replacing exons 13–16 with a neomycin resistance cassette (8). BTBR, *Fmr1^{-/-}* (*Fmr1* KO), and *Shank3b^{-/-}* (*Shank3b* KO) were used as test animals. C57BL6/J mice were used as controls for BTBR mice, wildtype littermates for *Fmr1* KO and *Shank3b* KO. Breeding was approved by the local authorities. Since ASD shows a higher prevalence in male individuals, only male mice were used in the experiments (1). The number of animals tested in each experiment is reported in every figure legend and in the results section. All the experiments were performed according to guidelines

TABLE 1 Receptor binding protocols for the [³H] ligands with competitors (noted with *) and incubation conditions.

Receptor-[³ H] ligand	Procedure	Incubation buffer	Time/Temperature
AMPA-[³ H]AMPA	Pre-incubation	50 mM Trisacetat (pH 7.2)	3 × 10 min at 4°C
	Main incubation	50 mM Trisacetat (pH 7.2) + 100 mM KSCN + 10 nM [³ H]AMPA + 10 M Quisqualate*	45 min at 4°C
	1st Rinsing	50 mM Trisacetat (pH 7.2)	3 × 4 s at 4°C
	2nd Rinsing	2.5% Glutaraldehyd in Acetone	2 × 2 s
NMDA-[³ H]MK-801	Pre-incubation	50 mM Tris-HCl (pH 7.2) + 50 μM Glutamate	15 min at 4°C
	Main incubation	50 mM Tris-HCl (pH 7.2) + 50 μM Glutamate + 30 μM Glycin + 50 μM Spermidin + 5 nM [³ H]MK-801 + 100 μM MK-801*	60 min at room temperature
	1st Rinsing	50 mM Tris-HCl (pH 7.2) + 50 μM Glutamate	2 × 5 min at 4°C
	2nd Rinsing	Distilled Water	2 × 5 min at 4°C
GABA _A -[³ H]Muscimol	Pre-incubation	50 mM Trisodium Citrate (pH 7.0)	3 × 5 min at 4°C
	Main incubation	50 mM Trisodium Citrate (pH 7.0) + 7.7 nM [³ H]Muscimol + 10 mM GABA*	40 min at 4°C
	Rinsing	50 mM Trisodium Citrate (pH 7.0)	3 × 3 s at 4°C

of the central animal facility institution (TARC, Mainz University Medical Center) representing those of the German Animal Welfare Act and the European Directive 2010/63/EU for the protection of animals used for scientific purposes. Reporting was carried out according to the ARRIVE guidelines for reporting *in vivo* experiments.

Tissue collection and processing

Mice were decapitated and brains were rapidly frozen in isopentane. They were further stored at -80°C until cutting. Brain slices were serially cut (20 μm thickness) in the coronal plane with a cryostat microtome (Leica, Germany). Slices containing Cer were cut similarly in the sagittal plane. The following bregma points were chosen for the analysis: 1.93 mm for the PFC, between 1.53 mm and 0.97 mm for DS and VS, -1.55 mm for the DH. Sagittal sections cut 0.72 mm lateral to the midline were considered for the Cer. For the location of the regions of interest, we referred to Paxinos and Franklin (22).

Totally, for each region of interest, 5 slices were collected and stored at -80°C until further histological and autoradiographic experiments. The first two slices were used for histological staining, the successive two were incubated with the [³H]-labeled ligands for AMPA, NMDA and GABA_A receptors. Slices containing Cer were incubated only with the [³H]-labeled ligands for GABA_A receptor. Indeed, as already shown, [³H]MK-801 yields no signal in the Cer at the concentrations used in this study (23).

Histology

Hematoxylin–eosin staining was performed to help spatially localize the regions of interest on the autoradiograms. Briefly, the frozen brain slices were acclimatized at room temperature for 10 min. The slices were then incubated in acetone for 5 min, briefly air dried, and dipped in hematoxylin (Thermo Fisher) for 1 min. After washing in running water for 10 min, the slices were put for 10 s in Eosin Y (Thermo Fisher). Then, the slices were dehydrated in increasing

ethanol concentrations (96 and 100%) each for 2 min. Finally, the slices were placed for 3 min in xylol, and cover slipped with Cytoseal XYL (Thermo Fisher). Pictures were scanned at 4× magnification with a Leica microscope (Leica, Germany), digitized and transferred to the MCID program.

In vitro receptor autoradiography

The receptor binding density for AMPA, NMDA, and GABA_A receptors was adapted from the protocols described in (24). The tritiated ligands [³H]AMPA, [³H]MK-801, and [³H]Muscimol were purchased from PerkinElmer (Germany). AMPA is an agonist of the homonymous receptor, MK-801, also known as dizocilpine, is an uncompetitive antagonist of the NMDA receptor and Muscimol is an agonist of the GABA_A receptor. In the first step, the pre-incubation, endogenous ligands were washed off. In the following main incubation, the tritiated ligands were incubated both in the presence of a competitor, in order to determine the unspecific binding, and without it, in order to assess the total binding. Finally, the slices were rinsed. The slices incubated with [³H]AMPA were additionally dried with a warm air stream for 2 s and afterwards with a cold air stream. Slices incubated with [³H]MK-801 and [³H]Muscimol were dried with a cold air stream. A detailed description of the protocols used is reported in Table 1.

Image acquisition and analysis

Image acquisition and analysis were performed as described in (25). [³H] plastic standards (Microscales®, Amersham, Freiburg, Germany) were exposed together with the tritium-labeled sections to a [³H]-sensitive film (Bio Max MR-1 Autoradiography Film, KODAKTM) for 12 ([³H]AMPA and [³H]Muscimol) and 15 ([³H]MK-801) weeks. The autoradiograms and the standards were scanned in equal lighting conditions with the digital CoolSNAP camera (Roper Scientific, Photometrics CoolSNAPTM cf., Ottobrunn/Munich Germany) and digitized with the MCID image analysis system (Imaging Research Inc., St. Catharines, Ontario,

Canada). The standards were used to calculate the relationship between the gray values of the autoradiograms and the concentration of radioactivity. Total binding was calculated on the autoradiograms on both hemispheres in the regions of interest after tracing their boundary on the hematoxylin–eosin staining (Figure 1). The unspecific binding was consistently slightly above background signal or completely lacking. The value was then subtracted from the total binding. The binding values obtained from each ligand were used to calculate in the DH the E/I ratio as follows: $(MK-801 + AMPA) / Muscimol$ (26).

Statistical analysis

Statistical analysis was carried out with Prism (GraphPad, Version 9) and Microsoft Excel. Normal distribution of the data was assessed through the D'Agostino-Pearson test. Outliers were screened with the Rout test. Student's multiple *t*-test was then performed. Raw *p*-values were then adjusted for multiple comparisons using the FDR correction method as described in (27). $p < 0.05$ was taken as threshold for statistical significance and results are shown as the mean \pm SEM. The experiments were

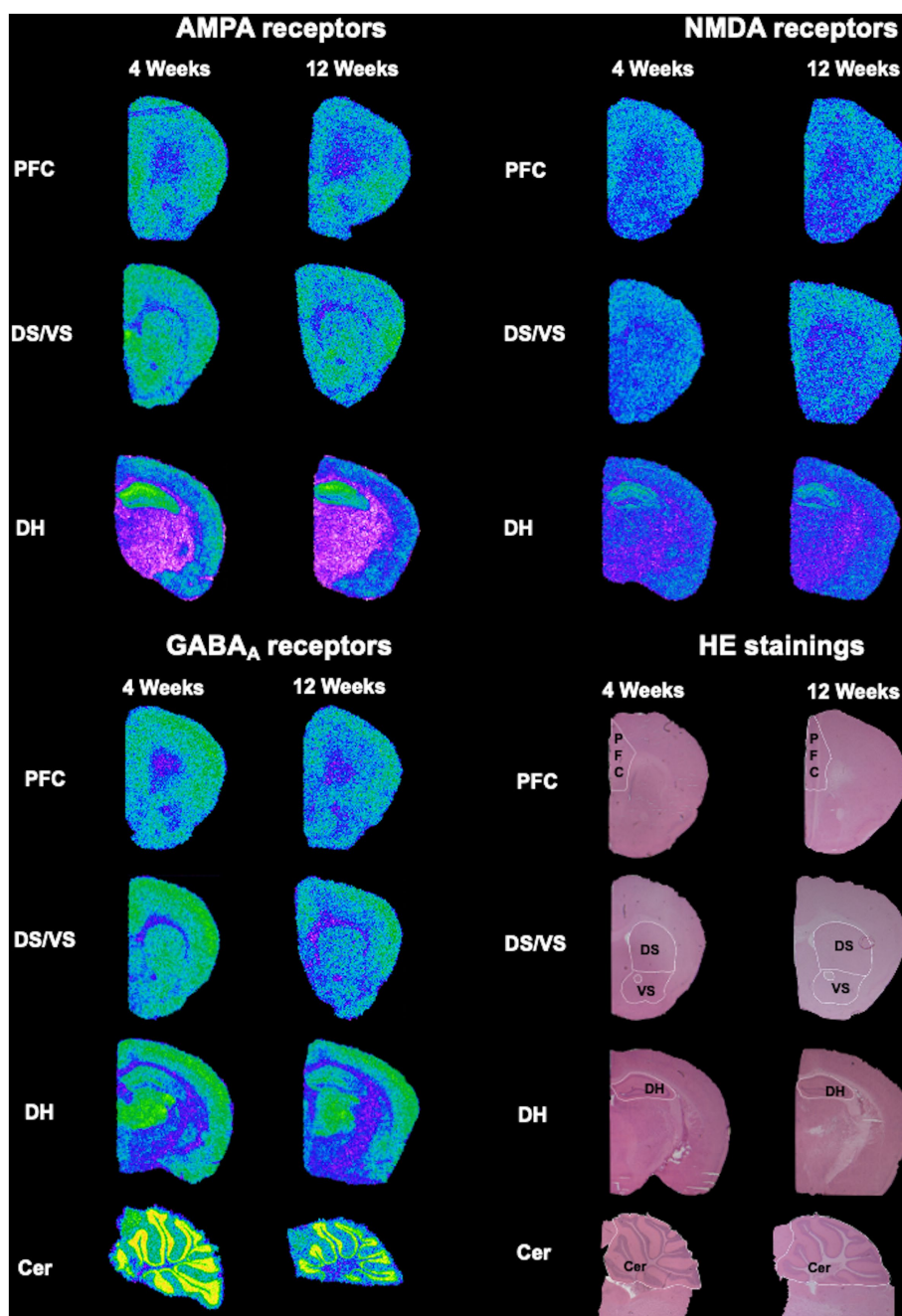


FIGURE 1

Exemplary overview of the autoradiograms and HE-stained sections. Slices stained with HE were used to trace the regions of interest (PFC, DS, VS, DH, and Cer), which were later overlaid on the respective autoradiograms for AMPA, NMDA and GABA_A receptors.

performed in a blinded manner and data are expressed as percentage of controls.

Results

This dataset describes alterations in receptor binding densities to AMPA, NMDA, and GABA_A receptors in PFC, DH, DS, VS, and Cer. It was obtained by means of quantitative *in vitro* receptor autoradiography of 4- and 12 week-old BTBR, *Fmr1* KO and *Shank3b* KO mice. Representative HE-stained sections were used to trace the boundaries of the above-mentioned regions of interest, which were then overlapped on the autoradiograms for AMPA, NMDA, and GABA_A receptors prior to analysis (Figure 1).

In BTBR mice, receptor binding density to AMPA receptors was significantly increased at DS and VS at 4 weeks (DS, $p=0.003$; VS, $p=0.025$) and a similar tendency was observed at 12 weeks (DS, $p=0.087$; VS, $p=0.087$) of age. However, no significant alterations were observed in PFC (4 weeks, $p=0.980$; 12 weeks, $p=0.612$) and DH (4 weeks, $p=0.485$; 12 weeks, $p=0.650$) at both time points (Figures 2A,B). Interestingly, binding density to NMDA receptors also showed a significant increase in DS at 4 weeks ($p=0.025$), but neither in VS ($p=0.102$) nor in both striatal subregions at adulthood (DS, $p=0.383$; VS, $p=0.299$). There was no change in AMPA or NMDA receptor binding in PFC (4 weeks, $p=0.316$; 12 weeks, $p=0.299$) and DH (4 weeks, $p=0.980$; 12 weeks, $p=0.979$) at both time points (Figures 2C,D). Furthermore, receptor binding density to GABA_A receptors was not changed in PFC at both 4 weeks ($p=0.092$) and 12 weeks ($p=0.158$). In DS and Cer a tendency to reduced receptor binding density was found at 4 weeks (DS, $p=0.081$; Cer, $p=0.081$) but was not observed at adulthood (DS, $p=0.802$; Cer, $p=0.299$). GABA_A receptor binding density in VS showed no change at both time points (4 weeks, $p=0.980$, 12 weeks, $p=0.979$). Notably, a strong propensity to increased GABA_A receptor binding density was found at 4 weeks ($p=0.069$), and it became significantly increased at 12 weeks ($p=0.003$) of age in DH (Figures 2E,F). Taken together, both glutamatergic and GABAergic receptors demonstrate discrete changes in receptor binding densities. Still, we found the most prominent differences persisting during development in the binding to AMPA receptors in DS and VS (increased) and to GABA_A receptors in DH (increased).

Fmr1 KO mice showed a propensity to increased binding density to AMPA receptors in PFC at 12 ($p=0.063$) but not 4 weeks ($p=0.156$). In DH we found the opposite, with a tendency to reduced receptor binding density at 12 ($p=0.059$) but not at 4 weeks ($p=0.156$). DS and VS showed no significant alterations at either time point (DS 4 weeks, $p=0.473$; VS 4 weeks, $p=0.641$; DS 12 weeks, $p=0.493$; VS 12 weeks, $p=0.632$) (Figures 3A,B). Binding density to NMDA receptors in PFC remained unchanged at both time points (4 weeks $p=0.373$; 12 weeks, $p=0.729$). In DS and VS, age dependent alterations are highlighted, with no change in receptor binding profile at 4 weeks (DS, $p=0.804$; VS, $p=0.533$) but reduced receptor binding densities at adulthood (DS, $p=0.058$; VS, $p=0.049$). DH showed reduced binding densities to NMDA receptors at both time points (4 weeks, $p=0.002$; 12 weeks, $p=0.058$) (Figures 3C,D). Regarding GABA_A receptors, binding density remained unaltered in PFC at 4 weeks ($p=0.473$) but showed significant reduction at 12 weeks ($p=0.049$). Similarly, no change was observed in DH at 4 weeks ($p=0.373$), whereas it was strongly

increased at adulthood ($p=0.025$). Binding profile of DS and VS remained unchanged at both time points (DS 4 weeks, $p=0.984$; VS 4 weeks, $p=0.473$; DS 12 weeks, $p=0.632$; VS 12 weeks, $p=0.729$). Strikingly, binding density to GABA_A receptor was significantly reduced in Cer at both 4 ($p=0.0009$) and 12 weeks ($p=0.049$) (Figures 3E,F). Collectively, *Fmr1* KO mice showed several alterations, which remained consistent with development, such as NMDA binding in DH (decreased) and GABA_A binding in Cer (decreased).

Interesting similarities regarding GABA_A receptor binding density can be observed both in the BTBR and *Fmr1* KO mice. At 4 weeks, it was decreased in Cer (strong tendency in BTBR and significant change in *Fmr1* KO mice), whereas it was increased in DH at adulthood. This evidence highlights that the ionotropic neurotransmitter receptors analyzed might be discretely altered in different regions.

In *Shank3b* KO mice no change was found for AMPA receptor binding density for all regions analyzed, both at 4 (PFC, $p=0.852$; DS, $p=0.583$; VS, $p=0.772$; DH, $p=0.442$) and 12 weeks (PFC, $p=0.692$; DS, $p=0.971$; VS, $p=0.896$; DH, $p=0.896$), respectively (Figures 4A,B). Interestingly, binding density to NMDA receptors showed no change in DS and VS at 4 (DS, $p=0.146$; VS, $p=0.146$) but a significant reduction at 12 weeks (DS, $p=0.016$; VS, $p=0.016$). However, no significant alterations were observed at both time points in PFC (4 weeks, $p=0.442$; 12 weeks, $p=0.971$) and DH (4 weeks, $p=0.442$; 12 weeks, $p=0.971$) (Figures 4C,D). Concerning GABA_A receptors, at both time points considered, no change was noticed in PFC (4 weeks, $p=0.583$; 12 weeks, $p=0.971$), DS (4 weeks, $p=0.442$; 12 weeks, $p=0.692$), and VS (4 weeks, $p=0.188$; 12 weeks, $p=0.896$). Finally, no change was observed at 4 weeks in DH ($p=0.852$) and Cer ($p=0.852$), whereas at 12 weeks the receptor binding density showed strong tendencies to increase in DH ($p=0.068$) and decrease in Cer ($p=0.068$), respectively (Figures 4E,F). As already known from previous studies (28), knockdown of SHANK3 is associated to NMDA receptor reduction and hypofunction.

Remarkably, increased GABA_A receptor binding density at adulthood in the DH was discovered as point of commonality among all the ASD mouse models analyzed in this study. This also leads to a disbalance in the binding to ionotropic excitatory and inhibitory receptors estimated through the calculation of the corresponding binding density-related E/I ratio (Figure 5). Moreover, in a region-specific fashion, GABA_A receptor binding density was reduced in Cer both in *Shank3b* (strong tendency) and *Fmr1* KO mice at adulthood.

Discussion

In this study, we report for the first time the analysis of the binding density to the main ionotropic excitatory (AMPA and NMDA) and inhibitory (GABA_A) receptors at the synapse by the means of receptor autoradiography in three different ASD mouse models. For the analysis, we chose two developmental time points corresponding to late infancy (4 weeks) and early adulthood (12 weeks). It has indeed been shown that synaptic proteins go through dynamical regulation during postnatal development (29). This consideration holds true also for AMPA (30), NMDA (19, 31, 32), and GABA_A (33–37) receptors. The study was limited to brain regions, in which the association to ASD is long known. Aware of the controversial definition of the murine PFC (38), we analyzed a region corresponding to the anterior

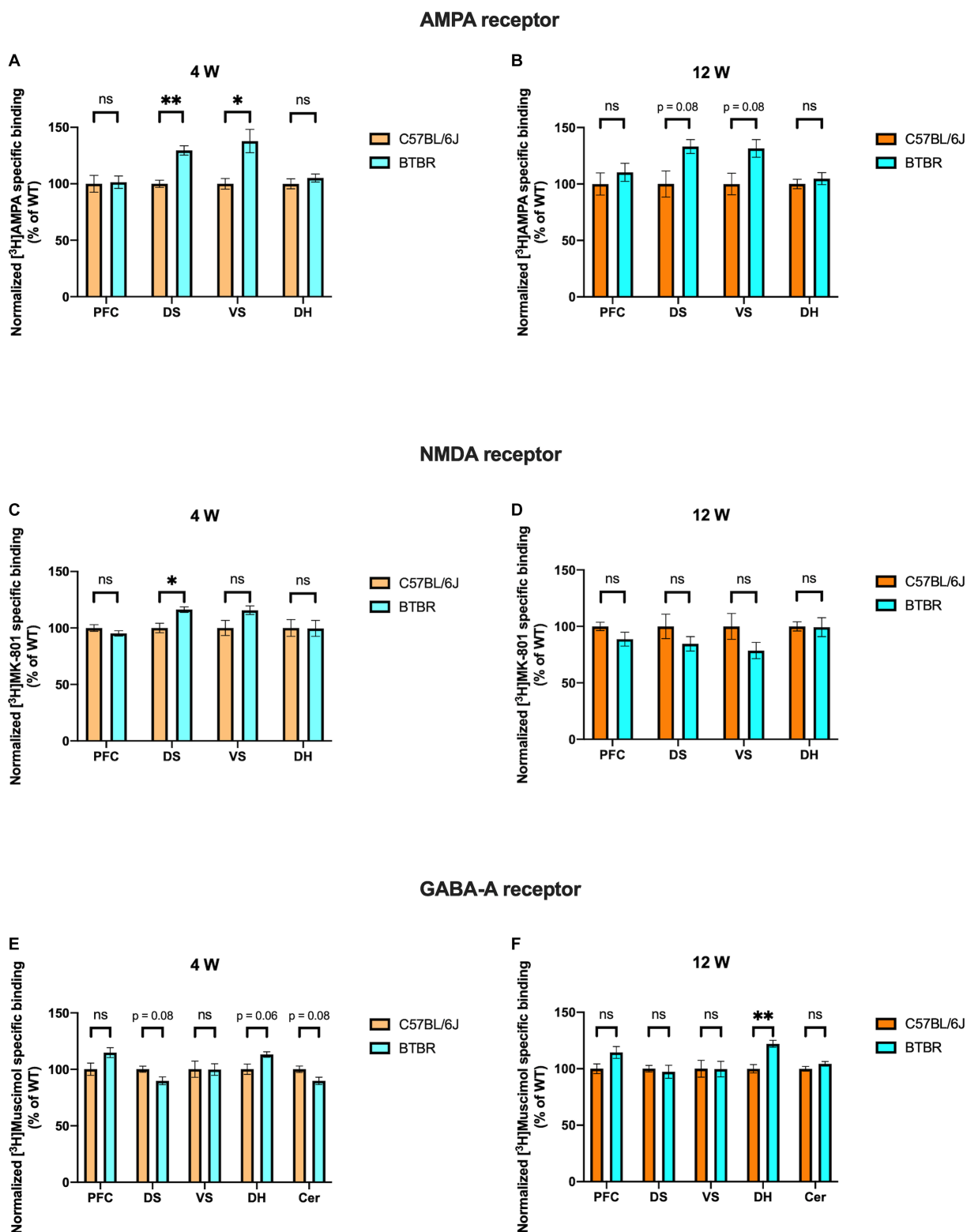


FIGURE 2 Bar charts representing mean and SEM of the receptor binding density in the BTBR line. Binding density to AMPA receptors at 4weeks (A) PFC: C57BL6/J (n=7), BTBR (n=6), DS: C57BL6/J (n=6), BTBR (n=6), VS: C57BL6/J (n=7), BTBR (n=7), DH: C57BL6/J (n=9), BTBR (n=10). Binding density to AMPA receptors at 12weeks (B) PFC: C57BL6/J (n=9), BTBR (n=9), DS: C57BL6/J (n=10), BTBR (n=10), VS: C57BL6/J (n=10), BTBR (n=10), DH: C57BL6/J (n=9), BTBR (n=10). Binding density to NMDA receptors at 4weeks (C) PFC: C57BL6/J (n=8), BTBR (n=8), DS: C57BL6/J (n=7), BTBR (n=8), VS: C57BL6/J (n=7), BTBR (n=7), DH: C57BL6/J (n=8), BTBR (n=9). Binding density to NMDA receptors at 12weeks (D) PFC: C57BL6/J (n=8), BTBR (n=10), DS: C57BL6/J (n=10), BTBR (n=10), VS: C57BL6/J (n=10), BTBR (n=10), DH: C57BL6/J (n=10), BTBR (n=10). Binding density to GABA_A receptors at 4weeks (E) PFC: C57BL6/J (n=8), BTBR (n=9), DS: C57BL6/J (n=8), BTBR (n=9), VS: C57BL6/J (n=7), BTBR (n=8), DH: C57BL6/J (n=9), BTBR (n=9),

(Continued)

FIGURE 2 (Continued)

Cer: C57BL6/J ($n=7$), BTBR ($n=7$). Binding density to GABA_A receptors at 12weeks (F) PFC: C57BL6/J ($n=9$), BTBR ($n=9$), DS: C57BL6/J ($n=10$), BTBR ($n=10$), VS: C57BL6/J ($n=10$), BTBR ($n=10$), DH: C57BL6/J ($n=9$), BTBR ($n=10$), Cer: C57BL6/J ($n=9$), BTBR ($n=9$). Significant differences are indicated with asterisks (* $p<0.05$ and ** $p<0.01$). Changes are represented as percentage of the mean of C57BL6/J mice.

cingulate, infralimbic and prelimbic cortex, as already previously shown (39). Frontal lobes in general, and PFC in particular, are known to play a role in complex social, cognitive, emotional and communicative skills (40). Str and NAcc are part of the basal ganglia and are functionally involved in the regulation of motor- and reward-motivated behavior (41). Although DH has been long associated to episodic memory and spatial orientations skills, recent acquisitions point at the involvement of this brain area in the development of the impaired social interaction phenotype typical of ASD (42). Finally, Cer is also embedded in the subcortical loops involved in the control of movement. Recent discoveries point out at the involvement of cerebellar projections to the emergence of social and cognitive impairment (43). Both macro- and microscopic alterations of the above-mentioned regions have been reported in ASD and have been hence selected for our screening (Figure 1) (44).

The E/I (excitation–inhibition) balance theory assumes that several psychiatric diseases, among which ASD, are due to a dysregulation of the excitatory and inhibitory factors existing at cellular, synaptic and circuit level, leading to a detrimental overall circuit activity (9, 16). Several factors contribute to the generation and maintenance of the E/I balance, such as glutamatergic and GABAergic ionotropic (AMPA, NMDA, GABA_A) and metabotropic receptors, signaling pathways, intrinsic neuronal excitability, homeostatic synaptic plasticity, interneurons, and glial cells (45, 46). Notably, disrupting the E/I balance in mice has been associated to the onset of impairments in social interaction (47). Moreover, additional ASD mouse models not investigated in this study such as, for example, *Nf1* KO (48), *Cntnap4* KO (49), and *Tsc1* KO mice (50) showed altered E/I balance. In the present study, attention was restricted to a singular factor contributing to the E/I balance, namely the analysis of the ionotropic receptors. Alterations of the ionotropic glutamatergic and GABAergic receptors in ASD models and patients are in part already known and will be hence here discussed. We need to point out though, that there has been little use so far of receptor autoradiography to evaluate the brain receptor distributions in ASD models, making the comparison with other studies, using different methodological approaches, difficult. Having the BTBR strain a very strong face validity for ASD, a great number of drugs was tested in this line. Knowledge about the mechanisms leading to the typical phenotypes of this line is still largely limited. Impairments in glutamatergic neurotransmission were demonstrated in cortical synaptoneuroosomes obtained from aged BTBR stimulated with potassium chloride (51). The use of AMPAKINE, positive modulators for AMPA receptors, in adult male and female BTBR mice led to improvement in social interaction and in learning and memory but not in the repetitive behavior (52). This is interesting to note, since we reported a significant increase of the AMPA binding density at 4 weeks and a strong tendency in the same direction at 12 weeks in the basal ganglia (Figures 2A,B), a region typically associated to the repetitive behavior phenotype, but not in the other regions considered. Increased D-aspartate, agonist of NMDA receptors, in PFC, hippocampus, and serum of BTBR, implicates alterations in the NMDA-related neurotransmission (53). Administration of D-cycloserine, a partial

agonist of the NMDA receptor, led to an improvement of the impaired social interaction phenotype (54). Furthermore memantine, an NMDA receptor antagonist, could reduce the repetitive behavior phenotype (55). For the first time, we provided a detailed neuroanatomical mapping of the NMDA receptor binding density in the BTBR line, highlighting increased binding at 4 weeks in the DS (Figure 2C). Moreover, increased levels of glutamate, glutamine and GABA_A were found in the Str of BTBR mice by the means of proton magnetic resonance spectroscopy (12). Reduced GABA_A mediated inhibitory transmission in the BTBR hippocampus at 3 weeks has been reported. Administration of L-838,417, a partial agonist specific for the GABA_A receptor subunits $\alpha 2$ and $\alpha 3$, proved efficacious in reducing the social impairment, whereas zolpidem, an $\alpha 1$ selective positive allosteric modulator, aggravated it (56). We showed at 12 weeks increased GABA_A receptor binding density in the DH (Figure 2F). A similar shift was observed also at 4 weeks (Figure 2E). These two observations should not be seen in contrast to each other since mutations in the scaffold protein gephyrin can lead to reduced GABAergic transmission in the presence of unchanged overall membrane expression (57, 58). Reduction of GABAergic transmission was moreover reported in the insular cortex of BTBR mice, resulting in defective multisensory integration. The deficit could be rescued with the application of diazepam, agonist at the benzodiazepine binding site of the GABA_A receptor (59). Successful application of diazepam in ameliorating the BTBR phenotype had already been reported (60). Other studies also showed the effects of drugs acting on the GABA_A-related system in male and female BTBR mice, such as gaboxadol, a potent GABA_A agonist, (61) and ganaxolone, a positive GABA_A allosteric modulator (62). In another study, a selective positive allosteric modulator of GABA_A receptor proved effective on adult male BTBR mice (63). Fragile X syndrome is the most common form of genetic intellectual disability and autism (64). The huge amount of evidence pertaining the synaptic function in the *Fmr1* KO model is therefore not surprising. In one report, reduced AMPA receptor subunit GluA1 was found in the cortex but not in the hippocampus and in the Cer of *Fmr1* KO mice, whereas no changes in NMDA receptor subunits were detected (65). Further evidence showed reduced levels of GluA1 phosphorylated at the serine 831 in the hippocampal dentate gyrus and cornu ammonis (66, 67). The phosphorylation of this amino acid is crucial for displaying normal long-term potentiation and long-term depression (68). In our hands, we found brain region-specific modifications, i.e., AMPA receptor binding density tended to increase in the PFC and to decrease in DH at 12 weeks in the *Fmr1* KO mice (Figure 3B). In another report, reduced GluN1, GluN2a, and GluN2b were detected in the PFC of *Fmr1* KO mice (69). In the dentate gyrus, impaired neurotransmission mediated from NMDA receptor was registered in multiple studies (66, 70–72). In one of them, moreover, the NMDA receptor subunits GluN1, GluN2a, and GluN2b were also found reduced in the dentate gyrus (66). We also found a consistent decrease of NMDA binding density at 4 weeks and a similar pattern at 12 weeks in the DH of *Fmr1* KO mice. Moreover, at 12 weeks significant reduction was also registered in DS and VS, whereas in the PFC no change was revealed.

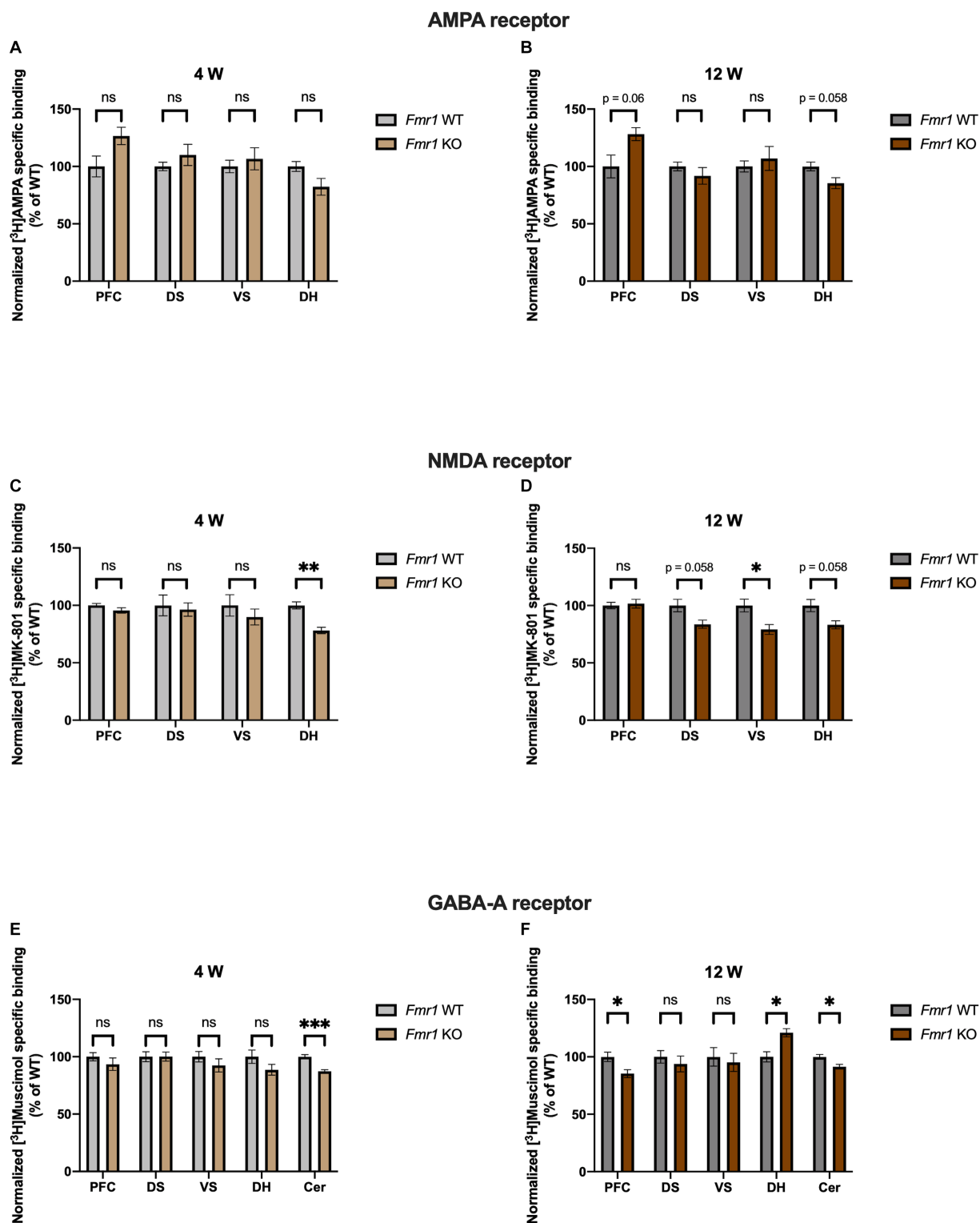


FIGURE 3 Bar charts representing mean and SEM of the receptor binding density in the *Fmr1* line. Binding density to AMPA receptors at 4 weeks (A) PFC: *Fmr1* WT ($n=8$), *Fmr1* KO ($n=7$), DS: *Fmr1* WT ($n=8$), *Fmr1* KO ($n=8$), VS: *Fmr1* WT ($n=9$), *Fmr1* KO ($n=8$), DH: *Fmr1* WT ($n=10$), *Fmr1* KO ($n=9$). Binding density to AMPA receptors at 12weeks (B) PFC: *Fmr1* WT ($n=7$), *Fmr1* KO ($n=6$), DS: *Fmr1* WT ($n=7$), *Fmr1* KO ($n=7$), VS: *Fmr1* WT ($n=7$), *Fmr1* KO ($n=6$), DH: *Fmr1* WT ($n=10$), *Fmr1* KO ($n=8$). Binding density to NMDA receptors at 4weeks (C) PFC: *Fmr1* WT ($n=7$), *Fmr1* KO ($n=8$), DS: *Fmr1* WT ($n=8$), *Fmr1* KO ($n=8$), VS: *Fmr1* WT ($n=8$), *Fmr1* KO ($n=7$), DH: *Fmr1* WT ($n=8$), *Fmr1* KO ($n=6$). Binding density to NMDA receptors at 12weeks (D) PFC: *Fmr1* WT ($n=8$), *Fmr1* KO ($n=8$), DS: *Fmr1* WT ($n=6$), *Fmr1* KO ($n=6$), VS: *Fmr1* WT ($n=7$), *Fmr1* KO ($n=6$), DH: *Fmr1* WT ($n=10$), *Fmr1* KO ($n=7$). Binding density to GABA_A receptors at 4weeks (E) PFC: *Fmr1* WT ($n=9$), *Fmr1* KO ($n=8$), DS: *Fmr1* WT ($n=9$), *Fmr1* KO ($n=7$), VS: *Fmr1* WT ($n=8$), *Fmr1* KO ($n=6$), DH: *Fmr1* WT ($n=10$), *Fmr1* KO ($n=7$), Cer: *Fmr1* WT ($n=9$), *Fmr1* KO ($n=8$). Binding density to GABA_A receptors at 12weeks (F) PFC: *Fmr1* WT ($n=7$), *Fmr1* KO ($n=8$), DS: *Fmr1* WT ($n=6$), *Fmr1* KO ($n=8$), VS: *Fmr1* WT ($n=6$), *Fmr1* KO ($n=8$), DH: *Fmr1* WT ($n=10$), *Fmr1* KO ($n=9$), Cer: *Fmr1* WT ($n=6$), *Fmr1* KO ($n=7$). Significant differences are indicated with asterisks (* $p<0.05$, ** $p<0.01$, and *** $p<0.001$). Changes are represented as percentage of the mean of *Fmr1* WT mice.

The differences found may be due to the dissimilarities among the experimental procedures performed in this and other studies (Figures 3C,D). Evidence about alterations of the GABAergic metabolism and neurotransmission is abundant (for a complete overview please refer to (73, 74)). mRNA levels of several GABA_A receptor subunits were found reduced in the cortex, but not in the hippocampus of *Fmr1* KO mice at 8–12 weeks (75). At 10 weeks of age, mRNA coding for several subunits of the GABA_A receptor were found reduced both in cortex and Cer (76). Analysis of full brain homogenates from *Fmr1* KO mice revealed, moreover, a tight temporal regulation, i.e., multiple GABA_A receptor subunits dysregulated at postnatal days 5 and 12 but not at early adulthood (77). In a previous report, the β subunit of the GABA_A receptor was found reduced in cortex, hippocampus, brainstem, and diencephalon but not in Cer of *Fmr1* KO mice at 8 weeks (78). Both $\alpha 2$ and $\beta 1$ GABA_A subunits were found reduced at mRNA and protein level in the hippocampus of animals at postnatal day 22 (79). The striking convergence among the different studies, is the reduction of the δ subunit of the GABA_A receptor (76, 77, 79, 80). GABA_A receptors, which contain the δ subunit, are only 5% of the total, are located perior extrasynaptically and mediate tonic inhibition (18, 81). In this study, the ligand [³H]Muscimol was used. It binds to the GABA binding site of the GABA_A receptor, which is to be found between the alpha and beta subunits. Hence, in the present study nothing can be inferred about the δ subunit. Moreover, at 4 weeks only GABA_A binding density in the Cer was strongly reduced (confirming the trend observed in the literature) (Figure 3E), whereas at 12 weeks GABA_A binding density showed region specific changes, being reduced in PFC and Cer and increased in DH (Figure 3F). Subsequently, drugs targeting GABA_A receptors such as benzodiazepines, ganaxolone and gaboxadol have been employed successfully in mice models of fragile X syndrome (82, 83).

Mutations in *SHANK3* account for up to 0.7% of cases of ASD and a multitude of mouse models have been generated so far (84, 85). Hence, evidence available in the literature does not always derive from the same mouse model we used. By the means of cell surface biotinylation assay, reduced AMPA and NMDA receptor subunits were detected in the *Shank3 $\alpha\beta$* KO model at 3–6 months in thalamus, hippocampus and striatum (86). In male and female *Shank3^{ex4-9}* KO mice, reduced GluA1 and GluN2a levels were registered (87). GluA2, GluN2a, and GluN2b were also found reduced in fractions obtained from the postsynaptic density of *Shank3b* KO mice (8). Interestingly, the use of an AMPAKINE and of D-cycloserine in *Shank3b* KO mice proved of limited efficacy (61). Although we found no changes regarding AMPA receptor binding density at both time points (Figures 4A,B), receptor binding to the NMDA receptor was reduced in DS and VS at adulthood (Figure 4D). Alterations of GABAergic markers were identified in pups and adult *Shank3b* KO mice (88). A recent study showed no significant changes regarding the binding availability to the benzodiazepine binding site of the GABA_A receptor both *in-vivo* on ASD patients (via PET scan) and *in-vitro* on ASD mouse models, among them *Shank3b* KO mice (via receptor autoradiography) (89). Of relevance, regarding binding density to the GABA_A receptor, we found a tendency to increase in the DH and decrease in the Cer at adulthood (Figure 4F). Discrepancies from the studies reported above might depend upon the different

ligands utilized. Finally, we intend to highlight the convergent increase at adulthood in DH of the GABA_A receptor binding densities in all the lines investigated (Figures 2F, 3F, 4F) and reduction in Cer in *Fmr1* KO and *Shank3b* KO lines (Figures 3E, 4F). The increased binding density to GABA_A also affects the receptor density-related balance between excitation and inhibition in the DH at adulthood (Figure 5).

Several lines of evidence deriving from human research point at a decisive involvement of the GABAergic system in ASD. Molecular studies revealed a downregulation of GABA_A receptor subunits in parts of the PFC and Cer (90–92). We also showed reduced binding density to the GABA_A receptor in the Cer (Figures 2E, 3E, 3F, 4F). Receptor autoradiography in parts of the PFC from ASD individuals, revealed reduced binding density to the GABA and benzodiazepine binding sites (93, 94), mirroring in part our results (Figure 3F). In the hippocampus of ASD patients, binding density to the benzodiazepine binding site was reduced (95). In another study, [³H]Muscimol binding was reduced in the pyramidal layer of CA1 but not changed in the remaining ones (96). Even if in this study the same ligand was used, values were measured on the whole DH as already performed by (97) and not on the individual layers. *In-vivo* PET studies also revealed reduced binding to the benzodiazepine binding site of the GABA_A receptor in patients affected by fragile X syndrome in one portion of the PFC (98), exactly as observed in the *Fmr1* KO mice at 12 weeks (Figure 3F). The generalized binding throughout the brain to receptors $\alpha 1$ and $\alpha 5$ of the GABA_A receptor was found reduced in ASD patients (99). Finally, a SPECT study in individuals with ASD showed a reduced accumulation of a radioactive ligand binding to the benzodiazepine binding site of the GABA_A receptor in the superior and medial frontal cortex (100). The abundant evidence available about disorders of the E/I balance in ASD is at the root of the numerous pharmacological attempts directed at its modulation (17, 101).

A limitation of the technical approach used in this study consists in the lack of cell specificity. Moreover, the results reported indicate the percentual change of receptors available, but nothing can be inferred about the functional state. In recent years, a growing body of evidence has put in relation altered inhibitory neurotransmission in ASD with parvalbumin (PV)-positive interneurons. Briefly, they are a class of GABAergic cortical and hippocampal interneurons expressing the calcium-binding protein parvalbumin and fine-tuning the E/I balance in the brain (102). Reports from human brains highlight region-specific changes in the number or density of PV-positive interneurons, being increased in the DH (103) and decreased in the PFC (104). Mice devoid of PV recapitulate all the typical hallmarks of ASD (105). Interestingly, all the ASD models investigated in this study show region-specific alterations of PV-positive interneurons (106–108).

Future studies should be directed at investigating the role of the E/I imbalance (109) or PV-positive cells (110). Taken together, our study highlights developmental and region-specific alterations of the ionotropic receptors landscape in ASD mouse models. We believe that *in-vitro* approaches such as patient-derived induced pluripotent stem cells, organoids and assembloids can further pave the way in both modelling neuropsychiatric conditions and testing potential drugs acting on these membrane receptors.

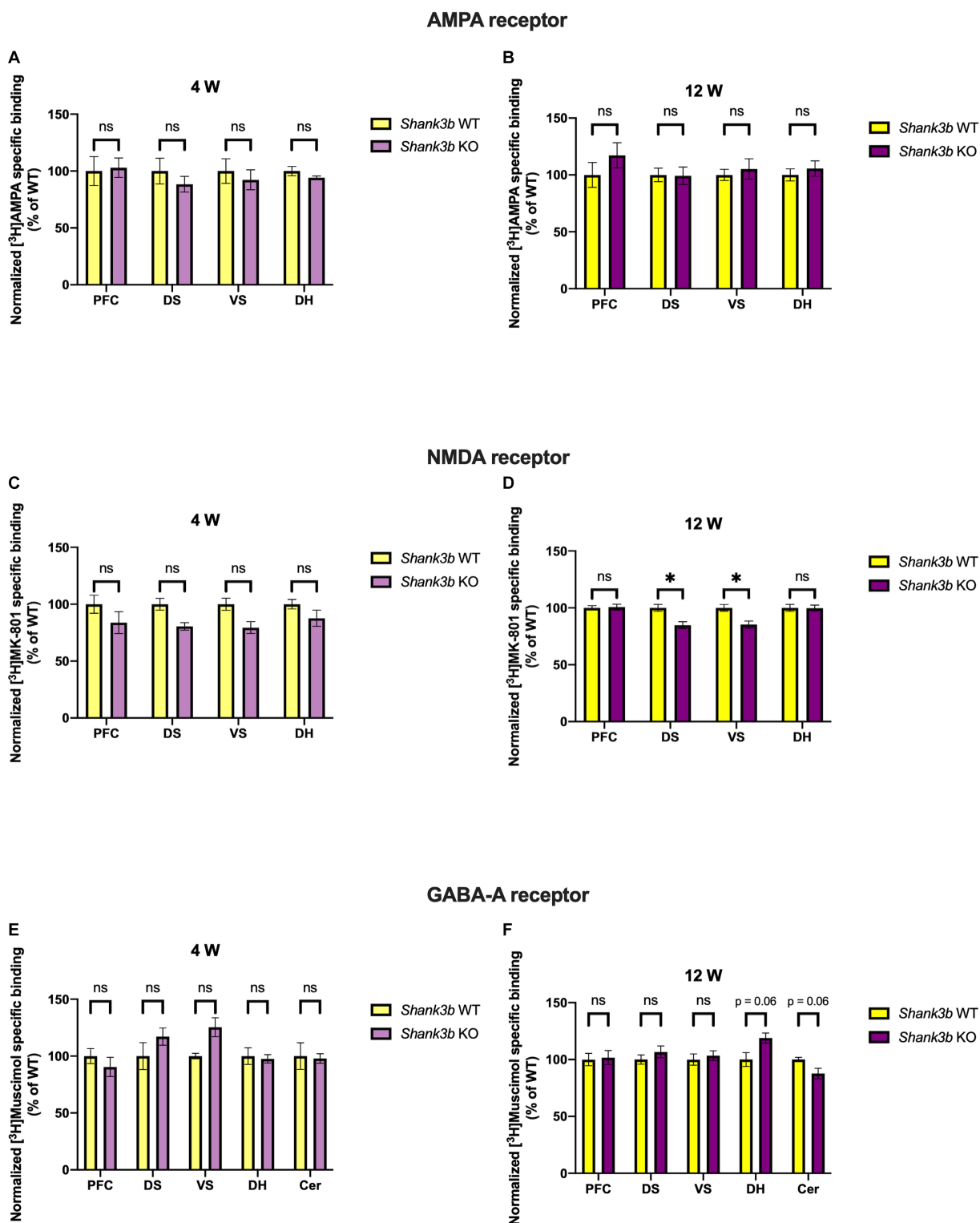


FIGURE 4
 Bar charts representing mean and SEM of the receptor binding density in the *Shank3b* line. Binding density to AMPA receptors at 4weeks (A) PFC: *Shank3b* WT (n=6), *Shank3b* KO (n=6), DS: *Shank3b* WT (n=6), *Shank3b* KO (n=6), VS: *Shank3b* WT (n=6), *Shank3b* KO (n=6), DH: *Shank3b* WT (n=5), *Shank3b* KO (n=5). Binding density to AMPA receptors at 12weeks (B) PFC: *Shank3b* WT (n=14), *Shank3b* KO (n=11), DS: *Shank3b* WT (n=15), *Shank3b* KO (n=10), VS: *Shank3b* WT (n=14), *Shank3b* KO (n=11), DH: *Shank3b* WT (n=14), *Shank3b* KO (n=12). Binding density to NMDA receptors at 4weeks (C) PFC: *Shank3b* WT (n=5), *Shank3b* KO (n=5), DS: *Shank3b* WT (n=6), *Shank3b* KO (n=5), VS: *Shank3b* WT (n=6), *Shank3b* KO (n=5), DH: *Shank3b* WT (n=6), *Shank3b* KO (n=6). Binding density to NMDA receptors at 12weeks (D) PFC: *Shank3b* WT (n=14), *Shank3b* KO (n=12), DS: *Shank3b* WT (n=14), *Shank3b* KO (n=12), VS: *Shank3b* WT (n=13), *Shank3b* KO (n=12), DH: *Shank3b* WT (n=14), *Shank3b* KO (n=11). Binding density to GABA_A receptors at 4weeks (E); PFC: *Shank3b* WT (n=6), *Shank3b* KO (n=6), DS: *Shank3b* WT (n=5), *Shank3b* KO (n=6), VS: *Shank3b* WT (n=4), *Shank3b* KO (n=6), DH: *Shank3b* WT (n=6), *Shank3b* KO (n=6), Cer: *Shank3b* WT (n=4), *Shank3b* KO (n=6). Binding density to GABA_A receptors at 12weeks (F) PFC: *Shank3b*

(Continued)

FIGURE 4 (Continued)

WT ($n=15$), *Shank3b* KO ($n=12$), DS: *Shank3b* WT ($n=15$), *Shank3b* KO ($n=12$), VS: *Shank3b* WT ($n=15$), *Shank3b* KO ($n=12$), DH: *Shank3b* WT ($n=13$), *Shank3b* KO ($n=12$), Cer: *Shank3b* WT ($n=11$), *Shank3b* KO ($n=11$). Significant differences are indicated with asterisks ($*p<0.05$). Changes are represented as percentage of the mean of *Shank3b* WT mice.

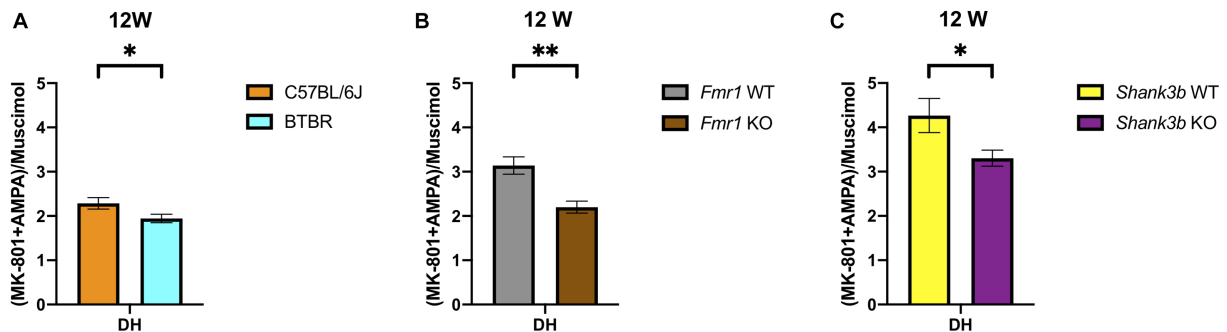


FIGURE 5

Bar charts representing mean and SEM of the receptor density-related E/I ratios from the DH of the three mouse lines analyzed in the study at 12 weeks of age. E/I ratio for at 12 weeks (A) DH: C57BL/6J ($n=8$), BTBR ($n=10$). E/I ratio for at 12 weeks (B) DH: *Fmr1* WT ($n=10$), *Fmr1* KO ($n=6$). E/I ratio for at 12 weeks (C) DH: *Shank3b* WT ($n=12$), *Shank3b* KO ($n=11$). Significant differences are indicated with asterisks ($*p<0.05$, $**p<0.01$).

Data availability statement

The raw data supporting the conclusions of this article will be made available by the authors, without undue reservation.

Ethics statement

Ethical review and approval was not required for the animal study because organ removal from mice for scientific purpose (the brain in this study) does not require approval by an ethics committee in Germany.

Author contributions

SC, LN, PL, CJS, and MJS planned the autoradiographic experiments. SC, LN, and PL conducted the autoradiographic experiments and analyzed the data. SC and LN drafted the manuscript. PL, DK-B, CJS, and MJS critically revised and edited the manuscript. All authors contributed to the article and approved the submitted version.

Funding

LN was supported by an internal grant of the University Medical Center, Mainz (Stufe I). MJS was supported by the

German Research Foundation (DFG, Collaborative Research Center 1080, Project B10) and the Werner Reichenberger Foundation. DK-B was supported by the Heisenberg program of the DFG (grant KR 5329/1-1).

Acknowledgments

The authors would like to thank Magdeleine Herkt, Christine Oswald and Alexander Wenzel for finest technical assistance and Frank Bicker for intense scientific discussion.

Conflict of interest

The authors declare that the research was conducted in the absence of any commercial or financial relationships that could be construed as a potential conflict of interest.

Publisher's note

All claims expressed in this article are solely those of the authors and do not necessarily represent those of their affiliated organizations, or those of the publisher, the editors and the reviewers. Any product that may be evaluated in this article, or claim that may be made by its manufacturer, is not guaranteed or endorsed by the publisher.

References

1. Lord C, Brugha TS, Charman T, Cusack J, Dumas G, Frazier T, et al. Autism spectrum disorder. *Nat Rev Dis Primers*. (2020) 6:5. doi: 10.1038/s41572-019-0138-4
2. Zeidan J, Fombonne E, Scora J, Ibrahim A, Durkin MS, Saxena S, et al. Global prevalence of autism: a systematic review update. *Autism Res*. (2022) 15:778–90. doi: 10.1002/aur.2696

3. Dietz PM, Rose CE, McArthur D, Maenner M. National and State estimates of adults with autism Spectrum disorder. *J Autism Dev Disord.* (2020) 50:4258–66. doi: 10.1007/s10803-020-04494-4
4. Casanova MF, Casanova EL, Frye RE, Baeza-Velasco C, LaSalle JM, Hagerman RJ, et al. Editorial: secondary vs. idiopathic autism. *Front Psych.* (2020) 11:297. doi: 10.3389/fpsy.2020.00297
5. Carroll L, Braeutigam S, Dawes JM, Krsnik Z, Kostovic I, Coutinho E, et al. Autism spectrum disorders: multiple routes to, and multiple consequences of, abnormal synaptic function and connectivity. *Neuroscientist.* (2021) 27:10–29. doi: 10.1177/1073858420921378
6. Meyza KZ, Blanchard DC. The BTBR mouse model of idiopathic autism - current view on mechanisms. *Neurosci Biobehav Rev.* (2017) 76:99–110. doi: 10.1016/j.neubiorev.2016.12.037
7. Bernardet M, Crusio WE. Fmr1 KO mice as a possible model of autistic features. *ScientificWorldJournal.* (2006) 6:1164–76. doi: 10.1100/tsw.2006.220
8. Peca J, Feliciano C, Ting JT, Wang W, Wells MF, Venkatraman TN, et al. Shank3 mutant mice display autistic-like behaviours and striatal dysfunction. *Nature.* (2011) 472:437–42. doi: 10.1038/nature09965
9. Rubenstein JL, Merzenich MM. Model of autism: increased ratio of excitation/inhibition in key neural systems. *Genes Brain Behav.* (2003) 2:255–67. doi: 10.1034/j.1601-183x.2003.00037.x
10. Chattopadhyaya B, Cristo GD. GABAergic circuit dysfunctions in neurodevelopmental disorders. *Front Psych.* (2012) 3:51. doi: 10.3389/fpsy.2012.00051
11. Eltokhi A, Santuy A, Merchan-Perez A, Sprengel R. Glutamatergic dysfunction and synaptic ultrastructural alterations in schizophrenia and autism Spectrum disorder: evidence from human and rodent studies. *Int J Mol Sci.* (2020) 22:59. doi: 10.3390/ijms22010059
12. Horder J, Petrinovic MM, Mendez MA, Bruns A, Takumi T, Spooren W, et al. Glutamate and GABA in autism spectrum disorder—a translational magnetic resonance spectroscopy study in man and rodent models. *Transl Psychiatry.* (2018b) 8:106. doi: 10.1038/s41398-018-0155-1
13. Manyukhina VO, Prokofyev AO, Galuta IA, Goiaeva DE, Obukhova TS, Schneiderman JF, et al. Globally elevated excitation–inhibition ratio in children with autism spectrum disorder and below-average intelligence. *Mol Autism.* (2022) 13:20. doi: 10.1186/s13229-022-00498-2
14. Port RG, Oberman LM, Roberts TP. Revisiting the excitation/inhibition imbalance hypothesis of ASD through a clinical lens. *Br J Radiol.* (2019) 92:20180944. doi: 10.1259/bjr.20180944
15. Zhao H, Mao X, Zhu C, Zou X, Peng F, Yang W, et al. GABAergic system dysfunction in autism spectrum disorders. *Front Cell Dev Biol.* (2021) 9:781327. doi: 10.3389/fcell.2021.781327
16. Sohal VS, Rubenstein JLR. Excitation–inhibition balance as a framework for investigating mechanisms in neuropsychiatric disorders. *Mol Psychiatry.* (2019) 24:1248–57. doi: 10.1038/s41380-019-0426-0
17. Canitano R, Palumbi R. Excitation/inhibition modulators in autism Spectrum disorder: current clinical research. *Front Neurosci.* (2021) 15:753274. doi: 10.3389/fnins.2021.753274
18. Rudolph U, Knoflach F. Beyond classical benzodiazepines: novel therapeutic potential of GABA_A receptor subtypes. *Nat Rev Drug Discov.* (2011) 10:685–97. doi: 10.1038/nrd3502
19. Paoletti P, Bellone C, Zhou Q. NMDA receptor subunit diversity: impact on receptor properties, synaptic plasticity and disease. *Nat Rev Neurosci.* (2013) 14:383–400. doi: 10.1038/nrn3504
20. Henley JM, Wilkinson KA. Synaptic AMPA receptor composition in development, plasticity, and disease. *Nat Rev Neurosci.* (2016) 17:337–50. doi: 10.1038/nrn.2016.37
21. Bakker CE, Verheij C, Willemsen R, Vanderhelm R, Oerlemans F, Vermey M, et al. Fmr1 knockout mice - a model to study fragile-X mental-retardation. *Cells.* (1994) 78:23–33. doi: 10.1016/0092-8674(94)90569-X
22. Paxinos G, Franklin KBJ. *Paxinos and Franklin's the mouse brain in stereotaxic coordinates.* 5th Edn, San Diego: Elsevier Academic Press (2019).
23. Sakurai SY, Cha JH, Penney JB, Young AB. Regional distribution and properties of [³H]MK-801 binding sites determined by quantitative autoradiography in rat brain. *Neuroscience.* (1991) 40:533–43. doi: 10.1016/0306-4522(91)90139-f
24. Frauenknecht K, Plaschke K, Sommer C. Transient oligemia is associated with long-term changes in binding densities of cortical inhibitory GABA_A receptors in the rat brain. *Brain Res.* (2009) 1271:95–102. doi: 10.1016/j.brainres.2009.03.028
25. Mammele S, Frauenknecht K, Sevimli S, Diederich K, Bauer H, Grimm C, et al. Prevention of an increase in cortical ligand binding to AMPA receptors may represent a novel mechanism of endogenous brain protection by G-CSF after ischemic stroke. *Restor Neurol Neurosci.* (2016) 34:665–75. doi: 10.3233/RNN-150543
26. Sommer C, Fahrner A, Kiessling M. [³H]muscimol binding to gamma-aminobutyric acid(a) receptors is upregulated in CA1 neurons of the gerbil hippocampus in the ischemia-tolerant state. *Stroke.* (2002) 33:1698–705. doi: 10.1161/01.str.0000016404.14407.77
27. Rosner B. *Fundamentals of biostatistics.* Cengage Learning, Inc (2011).
28. Duffney LJ, Wei J, Cheng J, Liu W, Smith KR, Kittler JT, et al. Shank3 deficiency induces NMDA receptor hypofunction via an actin-dependent mechanism. *J Neurosci.* (2013) 33:15767–78. doi: 10.1523/JNEUROSCI.1175-13.2013
29. Gonzalez-Lozano MA, Klemmer P, Gebuis T, Hassan C, van Nierop B, van Kesteren RE, et al. Dynamics of the mouse brain cortical synaptic proteome during postnatal brain development. *Sci Rep.* (2016) 6:35456. doi: 10.1038/srep35456
30. Blair MG, Nguyen NN, Albani SH, L'Etoile MM, Andrawis MM, Owen LM, et al. Developmental changes in structural and functional properties of hippocampal AMPARs parallels the emergence of deliberative spatial navigation in juvenile rats. *J Neurosci.* (2013) 33:12218–28. doi: 10.1523/JNEUROSCI.4827-12.2013
31. Monyer H, Burnashev N, Laurie DJ, Sakmann B, Seeburg PH. Developmental and regional expression in the rat brain and functional properties of four NMDA receptors. *Neuron.* (1994) 12:529–40. doi: 10.1016/0896-6273(94)90210-0
32. Watanabe M, Inoue Y, Sakimura K, Mishina M. Developmental changes in distribution of NMDA receptor channel subunit mRNAs. *Neuroreport.* (1992) 3:1138–40. doi: 10.1097/00001756-199212000-00027
33. Fritschy JM, Paysan J, Enna A, Mohler H. Switch in the expression of rat GABA_A-receptor subtypes during postnatal development: an immunohistochemical study. *J Neurosci.* (1994) 14:5302–24. doi: 10.1523/JNEUROSCI.14-09-05302.1994
34. Huntsman MM, Munoz A, Jones EG. Temporal modulation of GABA(a) receptor subunit gene expression in developing monkey cerebral cortex. *Neuroscience.* (1999) 91:1223–45. doi: 10.1016/s0306-4522(98)00713-1
35. Laurie DJ, Seeburg PH, Wisden W. The distribution of 13 GABA_A receptor subunit mRNAs in the rat brain. II. Olfactory bulb and cerebellum. *J Neurosci.* (1992a) 12:1063–76. doi: 10.1523/JNEUROSCI.12-03-01063.1992
36. Laurie DJ, Wisden W, Seeburg PH. The distribution of thirteen GABA_A receptor subunit mRNAs in the rat brain. III. Embryonic and postnatal development. *J Neurosci.* (1992b) 12:4151–72. doi: 10.1523/JNEUROSCI.12-11-04151.1992
37. Wisden W, Laurie DJ, Monyer H, Seeburg PH. The distribution of 13 GABA_A receptor subunit mRNAs in the rat brain. I. Telencephalon, diencephalon, mesencephalon. *J Neurosci.* (1992) 12:1040–62. doi: 10.1523/JNEUROSCI.12-03-01040.1992
38. Laubach M, Amarante LM, Swanson K, White SR. What, if anything, is rodent prefrontal cortex? *eNeuro.* (2018) 5:ENEURO.0315–18.2018. doi: 10.1523/ENEURO.0315-18.2018
39. Luo Y, Xiao Q, Wang J, Jiang L, Hu M, Jiang Y, et al. Running exercise protects oligodendrocytes in the medial prefrontal cortex in chronic unpredictable stress rat model. *Transl Psychiatry.* (2019) 9:322. doi: 10.1038/s41398-019-0662-8
40. Courchesne E, Pierce K. Why the frontal cortex in autism might be talking only to itself: local over-connectivity but long-distance disconnection. *Curr Opin Neurobiol.* (2005) 15:225–30. doi: 10.1016/j.comb.2005.03.001
41. Fuccillo MV. Striatal circuits as a common node for autism pathophysiology. *Front Neurosci.* (2016) 10:27. doi: 10.3389/fnins.2016.00027
42. Banker SM, Gu X, Schiller D, Foss-Feig JH. Hippocampal contributions to social and cognitive deficits in autism spectrum disorder. *Trends Neurosci.* (2021) 44:793–807. doi: 10.1016/j.tins.2021.08.005
43. van der Heijden ME, Gill JS, Sillitoe RV. Abnormal cerebellar development in autism Spectrum disorders. *Dev Neurosci.* (2021) 43:181–90. doi: 10.1159/000515189
44. Ecker C, Schmeisser MJ, Loth E, Murphy DG. Neuroanatomy and neuropathology of autism Spectrum disorder in humans. *Adv Anat Embryol Cell Biol.* (2017) 224:27–48. doi: 10.1007/978-3-319-52498-6_2
45. Lee E, Lee J, Kim E. Excitation/inhibition imbalance in animal models of autism Spectrum disorders. *Biol Psychiatry.* (2017) 81:838–47. doi: 10.1016/j.biopsych.2016.05.011
46. Lee EJ, Choi SY, Kim E. NMDA receptor dysfunction in autism spectrum disorders. *Curr Opin Pharmacol.* (2015) 20:8–13. doi: 10.1016/j.coph.2014.10.007
47. Yizhar O, Fenno LE, Prigge M, Schneider F, Davidson TJ, O'Shea DJ, et al. Neocortical excitation/inhibition balance in information processing and social dysfunction. *Nature.* (2011) 477:171–8. doi: 10.1038/nature10360
48. Goncalves J, Violante IR, Sereno J, Leitao RA, Cai Y, Abrunhosa A, et al. Testing the excitation/inhibition imbalance hypothesis in a mouse model of the autism spectrum disorder: in vivo neurospectroscopy and molecular evidence for regional phenotypes. *Mol Autism.* (2017) 8:47. doi: 10.1186/s13229-017-0166-4
49. Karayannis T, Au E, Patel JC, Kruglikov I, Markx S, Delorme R, et al. Cntnap4 differentially contributes to GABAergic and dopaminergic synaptic transmission. *Nature.* (2014) 511:236–40. doi: 10.1038/nature13248
50. Bateup HS, Johnson CA, Deneff CL, Saulnier JL, Kornacker K, Sabatini BL. Excitatory/inhibitory synaptic imbalance leads to hippocampal hyperexcitability in mouse models of tuberous sclerosis. *Neuron.* (2013) 78:510–22. doi: 10.1016/j.neuron.2013.03.017
51. Wei H, Ding C, Jin G, Yin H, Liu J, Hu F. Abnormal glutamate release in aged BTBR mouse model of autism. *Int J Clin Exp Pathol.* (2015) 8:10689–97.
52. Silverman JL, Oliver CF, Karras MN, Gastrell PT, Crawley JN. AMPAKINE enhancement of social interaction in the BTBR mouse model of autism. *Neuropharmacology.* (2013) 64:268–82. doi: 10.1016/j.neuropharm.2012.07.013

53. Nuzzo T, Sekine M, Punzo D, Miroballo M, Katane M, Saitoh Y, et al. Dysfunctional d-aspartate metabolism in BTBR mouse model of idiopathic autism. *Biochim Biophys Acta Proteins Proteom.* (2020) 1868:140531. doi: 10.1016/j.bbapap.2020.140531
54. Burket JA, Benson AD, Tang AH, Deutsch SI. D-Cycloserine improves sociability in the BTBR T+ Itpr3tf/J mouse model of autism spectrum disorders with altered Ras/Raf/ERK1/2 signaling. *Brain Res Bull.* (2013) 96:62–70. doi: 10.1016/j.brainresbull.2013.05.003
55. Eissa N, Venkatachalam K, Jayaprakash P, Falkenstein M, Dubiel M, Frank A, et al. The multi-targeting ligand ST-2223 with histamine H3 receptor and dopamine D2/D3 receptor antagonist properties mitigates autism-like repetitive behaviors and brain oxidative stress in mice. *Int J Mol Sci.* (2021) 22:1947. doi: 10.3390/ijms22041947
56. Han S, Tai C, Jones CJ, Scheuer T, Catterall WA. Enhancement of inhibitory neurotransmission by GABA_A receptors having alpha2,3-subunits ameliorates behavioral deficits in a mouse model of autism. *Neuron.* (2014) 81:1282–9. doi: 10.1016/j.neuron.2014.01.016
57. Kneussel M, Brandstatter JH, Laube B, Stahl S, Muller U, Betz H. Loss of postsynaptic GABA(a) receptor clustering in gephyrin-deficient mice. *J Neurosci.* (1999) 19:9289–97. doi: 10.1523/JNEUROSCI.19-21-09289.1999
58. Nelson SB, Valakh V. Excitatory/inhibitory balance and circuit homeostasis in autism Spectrum disorders. *Neuron.* (2015) 87:684–98. doi: 10.1016/j.neuron.2015.07.033
59. Gogolla N, Takesian AE, Feng G, Fagiolini M, Hensch TK. Sensory integration in mouse insular cortex reflects GABA circuit maturation. *Neuron.* (2014) 83:894–905. doi: 10.1016/j.neuron.2014.06.033
60. Defensor EB, Pearson BL, Pobbe RL, Bolivar VJ, Blanchard DC, Blanchard RJ. A novel social proximity test suggests patterns of social avoidance and gaze aversion-like behavior in BTBR T+ tf/J mice. *Behav Brain Res.* (2011) 217:302–8. doi: 10.1016/j.bbr.2010.10.033
61. Rhine MA, Parrott JM, Schultz MN, Kazdoba TM, Crawley JN. Hypothesis-driven investigations of diverse pharmacological targets in two mouse models of autism. *Autism Res.* (2019) 12:401–21. doi: 10.1002/aur.2066
62. Kazdoba TM, Hagerman RJ, Zolkowska D, Rogawski MA, Crawley JN. Evaluation of the neuroactive steroid ganaxolone on social and repetitive behaviors in the BTBR mouse model of autism. *Psychopharmacology.* (2016) 233:309–23. doi: 10.1007/s00213-015-4115-7
63. Yoshimura RF, Tran MB, Hogenkamp DJ, Ayala NL, Johnstone T, Dunnigan AJ, et al. Allosteric modulation of nicotinic and GABA_A receptor subtypes differentially modify autism-like behaviors in the BTBR mouse model. *Neuropharmacology.* (2017) 126:38–47. doi: 10.1016/j.neuropharm.2017.08.029
64. Hagerman RJ, Berry-Kravis E, Hazlett HC, Bailey DB, Moine H, Kooy RF, et al. Fragile X syndrome. *Nat Rev Dis Primers.* (2017) 3:17065. doi: 10.1038/nrdp.2017.65
65. Li J, Pelletier MR, Perez Velazquez JL, Carlen PL. Reduced cortical synaptic plasticity and GluR1 expression associated with fragile X mental retardation protein deficiency. *Mol Cell Neurosci.* (2002) 19:138–51. doi: 10.1006/mcne.2001.1085
66. Bostrom CA, Majaess NM, Morch K, White E, Eadie BD, Christie BR. Rescue of NMDAR-dependent synaptic plasticity in Fmr1 knock-out mice. *Cereb Cortex.* (2015) 25:271–9. doi: 10.1093/cercor/bht237
67. Hu H, Qin Y, Bochorishvili G, Zhu Y, van Aelst L, Zhu JJ. Ras signaling mechanisms underlying impaired GluR1-dependent plasticity associated with fragile X syndrome. *J Neurosci.* (2008) 28:7847–62. doi: 10.1523/JNEUROSCI.1496-08.2008
68. Lee HK, Takamiya K, He K, Song L, Hugarir RL. Specific roles of AMPA receptor subunit GluR1 (GluA1) phosphorylation sites in regulating synaptic plasticity in the CA1 region of hippocampus. *J Neurophysiol.* (2010) 103:479–89. doi: 10.1152/jn.00835.2009
69. Krueger DD, Osterweil EK, Chen SP, Tye LD, Bear MF. Cognitive dysfunction and prefrontal synaptic abnormalities in a mouse model of fragile X syndrome. *Proc Natl Acad Sci USA.* (2011) 108:2587–92. doi: 10.1073/pnas.1013855108
70. Eadie BD, Cushman J, Kannangara TS, Fanselow MS, Christie BR. NMDA receptor hypofunction in the dentate gyrus and impaired context discrimination in adult Fmr1 knockout mice. *Hippocampus.* (2012) 22:241–54. doi: 10.1002/hipo.20890
71. Yau SY, Bettio L, Chiu J, Chiu C, Christie BR. Fragile-X syndrome is associated with NMDA receptor hypofunction and reduced dendritic complexity in mature dentate granule cells. *Front Mol Neurosci.* (2018) 11:495. doi: 10.3389/fnfmol.2018.00495
72. Yun SH, Trommer BL. Fragile X mice: reduced long-term potentiation and N-methyl-D-aspartate receptor-mediated neurotransmission in dentate gyrus. *J Neurosci Res.* (2011) 89:176–82. doi: 10.1002/jnr.22546
73. Di J, Li J, O'Hara B, Alberts I, Xiong L, Li J, et al. The role of GABAergic neural circuits in the pathogenesis of autism spectrum disorder. *Int J Dev Neurosci.* (2020) 80:73–85. doi: 10.1002/jdn.10005
74. Paluszkiwicz SM, Martin BS, Huntsman MM. Fragile X syndrome: the GABAergic system and circuit dysfunction. *Dev Neurosci.* (2011) 33:349–64. doi: 10.1159/000329420
75. D'Hulst C, De Geest N, Reeve SP, Van Dam D, De Deyn PP, Hassan BA, et al. Decreased expression of the GABA_A receptor in fragile X syndrome. *Brain Res.* (2006) 1121:238–45. doi: 10.1016/j.brainres.2006.08.115
76. Braat S, D'Hulst C, Heulens I, De Rubeis S, Mientjes E, Nelson DL, et al. The GABA_A receptor is an FMRP target with therapeutic potential in fragile X syndrome. *Cell Cycle.* (2015) 14:2985–95. doi: 10.4161/15384101.2014.989114
77. Adusei DC, Pacey LK, Chen D, Hampson DR. Early developmental alterations in GABAergic protein expression in fragile X knockout mice. *Neuropharmacology.* (2010) 59:167–71. doi: 10.1016/j.neuropharm.2010.05.002
78. El Drissi A, Ding XH, Scalia J, Trenkner E, Brown WT, Dobkin C. Decreased GABA(a) receptor expression in the seizure-prone fragile X mouse. *Neurosci Lett.* (2005) 377:141–6. doi: 10.1016/j.neulet.2004.11.087
79. Sabanov V, Braat S, D'Andrea L, Willemsen R, Zeidler S, Rooms L, et al. Impaired GABAergic inhibition in the hippocampus of Fmr1 knockout mice. *Neuropharmacology.* (2017) 116:71–81. doi: 10.1016/j.neuropharm.2016.12.010
80. Gantois I, Vandesompele J, Speleman F, Reyniers E, D'Hooge R, Severijnen LA, et al. Expression profiling suggests underexpression of the GABA(a) receptor subunit delta in the fragile X knockout mouse model. *Neurobiol Dis.* (2006) 21:346–57. doi: 10.1016/j.nbd.2005.07.017
81. Zheleznova NN, Sedelnikova A, Weiss DS. Function and modulation of delta-containing GABA(a) receptors. *Psychoneuroendocrinology.* (2009) 34:S67–73. doi: 10.1016/j.psyneuen.2009.08.010
82. Cogram P, Deacon RMJ, Warner-Schmidt JL, von Schimmelmann MJ, Abrahams BS, Daring MJ. Gaboxadol normalizes behavioral abnormalities in a mouse model of fragile X syndrome. *Front Behav Neurosci.* (2019) 13:141. doi: 10.3389/fnbeh.2019.00141
83. Heulens I, D'Hulst C, Van Dam D, De Deyn PP, Kooy RF. Pharmacological treatment of fragile X syndrome with GABAergic drugs in a knockout mouse model. *Behav Brain Res.* (2012) 229:244–9. doi: 10.1016/j.bbr.2012.01.031
84. Leblond CS, Nava C, Polge A, Gauthier J, Huguet G, Lumbroso S, et al. Meta-analysis of SHANK mutations in autism Spectrum disorders: a gradient of severity in cognitive impairments. *PLoS Genet.* (2014) 10:e1004580. doi: 10.1371/journal.pgen.1004580
85. SFARI (2022). SHANK3 [Online]. Available at: <https://gene.sfari.org/database/animal-models/genetic-animal-models/SHANK3/Mus%20musculus#genetic-models-tab> (Accessed October 20, 2022).
86. Heise C, Preuss JM, Schroeder JC, Battaglia CR, Kolibius J, Schmid R, et al. Heterogeneity of cell surface glutamate and GABA receptor expression in shank and CNTN4 autism mouse models. *Front Mol Neurosci.* (2018) 11:212. doi: 10.3389/fnfmol.2018.00212
87. Wang X, McCoy PA, Rodriguiz RM, Pan Y, Je HS, Roberts AC, et al. Synaptic dysfunction and abnormal behaviors in mice lacking major isoforms of Shank3. *Hum Mol Genet.* (2011) 20:3093–108. doi: 10.1093/hmg/ddr212
88. Bukatova S, Renczes E, Reichova A, Filo J, Sadlonova A, Mravec B, et al. Shank3 deficiency is associated with altered profile of neurotransmission markers in pups and adult mice. *Neurochem Res.* (2021) 46:3342–55. doi: 10.1007/s11064-021-03435-6
89. Horder J, Andersson M, Mendez MA, Singh N, Tangen A, Lundberg J, et al. GABA_A receptor availability is not altered in adults with autism spectrum disorder or in mouse models. *Sci Transl Med.* (2018a) 10:eaam8434. doi: 10.1126/scitranslmed.aam8434
90. Blatt GJ, Fatemi SH. Alterations in GABAergic biomarkers in the autism brain: research findings and clinical implications. *Anat Rec.* (2011) 294:1646–52. doi: 10.1002/ar.21252
91. Fatemi SH, Reutiman TJ, Folsom TD, Rooney RJ, Patel DH, Thuras PD. mRNA and protein levels for GABA_Aalpha4, alpha5, beta1 and GABABR1 receptors are altered in brains from subjects with autism. *J Autism Dev Disord.* (2010) 40:743–50. doi: 10.1007/s10803-009-0924-z
92. Fatemi SH, Reutiman TJ, Folsom TD, Thuras PD. GABA(a) receptor downregulation in brains of subjects with autism. *J Autism Dev Disord.* (2009) 39:223–30. doi: 10.1007/s10803-008-0646-7
93. Oblak A, Gibbs TT, Blatt GJ. Decreased GABA_A receptors and benzodiazepine binding sites in the anterior cingulate cortex in autism. *Autism Res.* (2009) 2:205–19. doi: 10.1002/aur.88
94. Oblak AL, Gibbs TT, Blatt GJ. Reduced GABA_A receptors and benzodiazepine binding sites in the posterior cingulate cortex and fusiform gyrus in autism. *Brain Res.* (2011) 1380:218–28. doi: 10.1016/j.brainres.2010.09.021
95. Guptill JT, Booker AB, Gibbs TT, Kemper TL, Bauman ML, Blatt GJ. [³H]-flunitrazepam-labeled benzodiazepine binding sites in the hippocampal formation in autism: a multiple concentration autoradiographic study. *J Autism Dev Disord.* (2007) 37:911–20. doi: 10.1007/s10803-006-0226-7
96. Blatt GJ, Fitzgerald CM, Guptill JT, Booker AB, Kemper TL, Bauman ML. Density and distribution of hippocampal neurotransmitter receptors in autism: an autoradiographic study. *J Autism Dev Disord.* (2001) 31:537–43. doi: 10.1023/a:1013238809666
97. Behuet S, Cremer JN, Cremer M, Palomero-Gallagher N, Zilles K, Amunts K. Developmental changes of glutamate and GABA receptor densities in Wistar rats. *Front Neuroanat.* (2019) 13:100. doi: 10.3389/fnana.2019.00100

98. D'Hulst C, Heulens I, Van der Aa N, Goffin K, Koole M, Porke K, et al. Positron emission tomography (PET) quantification of GABAA receptors in the brain of fragile X patients. *PLoS One*. (2015) 10:e0131486. doi: 10.1371/journal.pone.0131486
99. Mendez MA, Horder J, Myers J, Coghlan S, Stokes P, Erritzoe D, et al. The brain GABA-benzodiazepine receptor alpha-5 subtype in autism spectrum disorder: a pilot [(11C)Ro15-4513 positron emission tomography study. *Neuropharmacology*. (2013) 68:195–201. doi: 10.1016/j.neuropharm.2012.04.008
100. Mori T, Mori K, Fujii E, Toda Y, Miyazaki M, Harada M, et al. Evaluation of the GABAergic nervous system in autistic brain: (123I)-iomazenil SPECT study. *Brain Dev*. (2012) 34:648–54. doi: 10.1016/j.braindev.2011.10.007
101. Brondino N, Fusar-Poli L, Panisi C, Damiani S, Barale F, Politi P. Pharmacological modulation of GABA function in autism spectrum disorders: a systematic review of human studies. *J Autism Dev Disord*. (2016) 46:825–39. doi: 10.1007/s10803-015-2619-y
102. Filice F, Janickova L, Henzi T, Bilella A, Schwaller B. The Parvalbumin hypothesis of autism spectrum disorder. *Front Cell Neurosci*. (2020a) 14:577525. doi: 10.3389/fncel.2020.577525
103. Lawrence YA, Kemper TL, Bauman ML, Blatt GJ. Parvalbumin-, calbindin-, and calretinin-immunoreactive hippocampal interneuron density in autism. *Acta Neurol Scand*. (2010) 121:99–108. doi: 10.1111/j.1600-0404.2009.01234.x
104. Hashemi E, Ariza J, Rogers H, Noctor SC, Martinez-Cerdeno V. The number of Parvalbumin-expressing interneurons is decreased in the prefrontal cortex in autism. *Cereb Cortex*. (2017) 27:1931–43. doi: 10.1093/cercor/bhw021
105. Wohr M, Orduz D, Gregory P, Moreno H, Khan U, Vorckel KJ, et al. Lack of parvalbumin in mice leads to behavioral deficits relevant to all human autism core symptoms and related neural morphofunctional abnormalities. *Transl Psychiatry*. (2015) 5:e525. doi: 10.1038/tp.2015.19
106. Briones BA, Pisano TJ, Pitcher MN, Haye AE, Diethorn EJ, Engel EA, et al. Adult-born granule cell mossy fibers preferentially target parvalbumin-positive interneurons surrounded by perineuronal nets. *Hippocampus*. (2021) 31:375–88. doi: 10.1002/hipo.23296
107. Filice F, Vorckel KJ, Sungur AO, Wohr M, Schwaller B. Reduction in parvalbumin expression not loss of the parvalbumin-expressing GABA interneuron subpopulation in genetic parvalbumin and shank mouse models of autism. *Mol Brain*. (2016) 9:10. doi: 10.1186/s13041-016-0192-8
108. Selby L, Zhang C, Sun QQ. Major defects in neocortical GABAergic inhibitory circuits in mice lacking the fragile X mental retardation protein. *Neurosci Lett*. (2007) 412:227–32. doi: 10.1016/j.neulet.2006.11.062
109. Culotta L, Penzes P. Exploring the mechanisms underlying excitation/inhibition imbalance in human iPSC-derived models of ASD. *Mol Autism*. (2020) 11:32. doi: 10.1186/s13229-020-00339-0
110. Filice F, Schwaller B, Michel TM, Grunblatt E. Profiling parvalbumin interneurons using iPSC: challenges and perspectives for autism spectrum disorder (ASD). *Mol Autism*. (2020b) 11:10. doi: 10.1186/s13229-020-0314-0

Glossary

[³ H]	tritium
AMPA	α -amino-3-hydroxy-5-methyl-4-isoxazolepropionic acid
ASD	autism spectrum disorders
Cer	cerebellum
BTBR	black and tan brachyury
DH	dorsal hippocampus
DS	dorsal striatum
E/I	excitation–inhibition
FMRI	fragile X messenger ribonucleoprotein 1
GABA	γ -Aminobutyric acid
KO	knockout
NMDA	N-methyl-D-aspartate
PV	parvalbumin
PFC	prefrontal cortex
SEM	standard error of the mean
SHANK	SH3 and multiple ankyrin repeat domains protein 3
VS	ventral striatum
VTA	ventral tegmental area
WT	wildtype.